PERGAMON

International Journal of Heat and Mass Transfer 45 (2002) 3725–3740

International Journal of HEAT and MASS TRANSFER

www.elsevier.com/locate/ijhmt

Double diffusion, natural convection in an enclosure filled with saturated porous medium subjected to cross gradients; stably stratified fluid

A.A. Mohamad [a,*], R. Bennacer [b]

[a] Department of Mechanical and Manufacturing Engineering, The University of Calgary, Calgary, AB, Canada T2N 1N4
[b] Université de Cergy-Pontoise LEEVAM- Neuville Sur Oise 95031, France

Received 26 October 2001; received in revised form 16 February 2002

Abstract

Two- and three-dimensional flows, heat and mass transfer in a horizontal enclosure with aspect ratio of two filled with saturated porous medium were analyzed numerically. The enclosure is heated differentially and stably stratified species concentration is imposed vertically. The Prandtl number is fixed to 10 (aqueous solutions). The Lewis number is varied in the range of 1.0–1000 to cover a wide range of species diffusion material in water. The work is concentrated on stable stratified flow. The results of two- and three-dimensional models were compared. Interesting results are obtained for a wide range of solutal to thermal buoyancy ratios. The difference in the rate of heat and mass transfer between prediction of three- and two-dimensional simulations is not that significant, even though the flow exhibits a three-dimensional structure. This is due to the fact that the spanwise flow is very weak when compared with main flow.

1. Introduction

Natural convective heat and mass transfer in a saturated porous medium in enclosures has numerous industrial and geophysical applications, such as petrochemical process, food industry, grain storages, electrochemical process, fuel cells, pollutant dispersions in soil and underground water. A comprehensive review of the literature on double diffusion, natural convection in saturated porous media may be found in [1–5]. As far as the relation between thermal and concentration buoyancy forces is concerned, the problem of double diffusion can be classified into the following categories. Heat and mass gradients are imposed horizontally along the enclosure, either aiding or opposing each other. The other category is that the heat and mass gradients are imposed vertically, again either aiding or opposing each other (modified Rayleigh–Benard convection; stratified medium). Both problems were extensively considered in the literature, and mostly it is assumed that the flow is two-dimensional [2–4,6–14]. Recently, Sezai and Mohamad [5], presented results for three-dimensional flow in a cubic cavity filled with porous medium and subjected to opposing thermal and concentration gradients. Their results revealed that for a certain range the controlling parameters of the flow become three-dimensional and multi-solution is possible within this range. Therefore, it is difficult to justify two-dimensional assumptions for that range of controlling parameters. Furthermore, the relation between thermal and concentration gradients can be categorized as a cross gradient relation, where the thermal and concentrations gradients are imposed vertically and horizontally, respectively, or vice versa. This kind of problem was recently considered by Mohamad and Bennacer [15] and Bennacer et al. [16]. They assumed that the flow is two-dimensional and the analysis was done for an enclosure with aspect ratio of two, $Pr = 0.71$, $Le = 10$, $Gr_T = 10^6$–10^8, $Da = 10^{-4}$–10^{-6} and for buoyancy ratio, $0.25 \leqslant N \leqslant 2.0$. Flow bifurcation is predicted for N value

* Corresponding author. Tel.: +1-403-220-2781; fax: +1-403-282-8406.
E-mail address: amohamad@enme.ucalgary.ca (A.A. Mohamad).

0017-9310/02/$ - see front matter
PII: S0017-9310(02)00093-5

Nomenclature

A	aspect ratio, $A = L/H$
C	dimensional solute concentration
D	mass diffusivity ($m^2\ s^{-1}$)
Da	Darcy number, K/H^2
g	gravitational acceleration ($m\ s^{-2}$)
Gr_S	solutal Grashof number, $g\beta_S\Delta CH^3/v^2$
Gr_T	thermal Grashof number, $g\beta_T\Delta TH^3/v^2$
H, L	height and length of the enclosure
K	permeability of the porous medium
Le	Lewis number, α/D
N	buoyancy ratio, $\beta_S\Delta C/\beta_T\Delta T$
Nu	average Nusselt number
P	dimensionless pressure
Pr	effective Prandtl number, v/α
Ra	modified thermal Rayleigh number, $Gr_T Pr\, Da$
Ra_T	thermal Rayleigh number, $Gr_T Pr$
Sc	effective Schmidt number, v/D
Sh	average Sherwood number
T	dimensional temperature (K)
$u(v)$	horizontal and vertical components of the velocity
$U(V)$	horizontal (vertical) dimensionless components of velocity, $uH/v(vH/v)$
x, y	coordinate system

Greek symbols

α	thermal diffusivity ($m^2\ s^{-1}$)
β_S	coefficient of density change due to concentration
β_T	coefficient of volumetric thermal expansion (K^{-1})
ϵ	porosity
$\eta, (\xi)$	dimensionless coordinate system, y/H, (x/H)
ϕ	dimensionless concentration, $(C - C_0)/\Delta C$
θ	dimensionless temperature, $(T - T_c)/\Delta T$
ΔC	concentration difference between horizontal boundaries, $C_1 - C_0$
ΔT	Temperature difference between vertical boundaries, $T_h - T_c$
μ	dynamic viscosity of the fluid ($kg\ m^{-1}\ s^{-1}$)
μ_{eff}	viscosity in the Brinkman model ($kg\ m^{-1}\ s^{-1}$)
v	kinematics viscosity ($m^2\ s^{-1}$)
ρ	fluid density ($kg\ m^{-3}$)

Subscripts

Eff	effective
Eq	equivalent
F	fluid
0	reference state
S	solutal
T	thermal

in the range of about 0.8–1.0. The bifurcation occurs when the concentration buoyancy force starts to overcome the thermally induced flow. One main circulation is predicated for thermally dominated flow and as the concentration gradients are increased to a limit, the thermally driven flow is suppressed and the flow breaks into two thermally driven circulations. These circulations exist near the horizontal boundaries. With further increase of concentration gradient (N), the flow is totally suppressed by strong stable concentration gradient and the flow may be channeled along the boundaries. Also, Bennacer et al. [16] explored the stability of the same problem, where oscillatory flow is predicted for a limited range of buoyancy ratios. The oscillatory flow is attributed to the interaction between concentration plumes and thermal cells.

In general, the geometrical, initial and boundary conditions symmetry is not a sufficient condition for the flow symmetry as explored by Sezia and Mohamad [5] for double diffusion problem in an enclosure subjected to opposing thermal and concentration buoyancy forces. Perfect symmetry is not possible in real systems due to defects in geometry, initial and boundary conditions. In numerical analysis, errors due to false diffusion, truncation and rounding off errors may become sources of asymmetry. Fluid dynamics is full of such problems, such as Rayleigh–Benard and Taylor–Couette flows. Therefore, there is a good reason to explore the possibility of three dimensions, which is more realistic, of the double diffusion in an enclosure subjected to cross gradients.

Isothermal stable or unstable stratification takes place in an enclosure subjected to positive or negative concentration gradient, respectively. Stable stratification produces linear diffusive gradient in the vertical direction and any perturbation in the initial or boundary conditions may be suppressed due to stratification. Heating the vertical boundary induces flow, which transfers high concentration parcels in the flow direction. These parcels may be carried to a region of low temperature and fluid starts descending before reaching the end of the enclosure. Hence, it is expected that the flow structure become complex and may be three-dimensional depending on the controlling parameters.

For isothermal unstable stratification (high concentration on top of low concentration), perturbation in the

initial or boundary conditions may be amplified and flow initiates in the cavity. Rolls or plums form above threshold concentration Rayleigh number (concentration Rayleigh–Bénard problem), i.e., the flow structure depends on the concentration Rayleigh number, geometry of the container and fluid properties. The flow structure becomes quite complex and a two-dimensional solution is difficult to justify. On the other hand, if a temperature gradient is imposed horizontally (differential heating), it may rearrange the structure of the flow, which depends on the thermal Rayleigh number and two-dimensional solution can be justified for a certain range of controlling parameters. It is worth mentioning that imposing horizontal temperature gradient may have similar effects of tilting the enclosure or shearing the lid of the cavity.

These problems (stable and unstable) have fundamental importance as well as applications in geophysics, oceanography and the industry. For instance, in fuel storage installations, heavy or light fuel leaks into the surrounding soil and any fire or heating sources nearby the system may initiate fire. Understanding such a problem is very important in fire control measures.

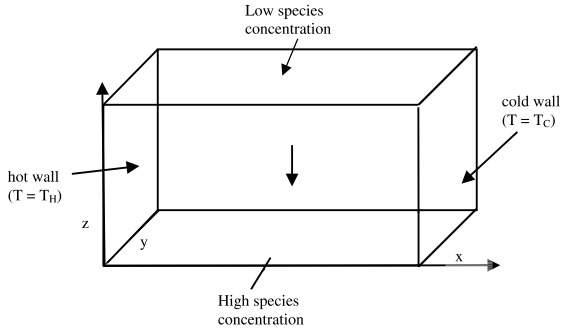

Fig. 1. Schematic diagram and the coordinate system for convection with horizontal temperature and vertical solutal gradient.

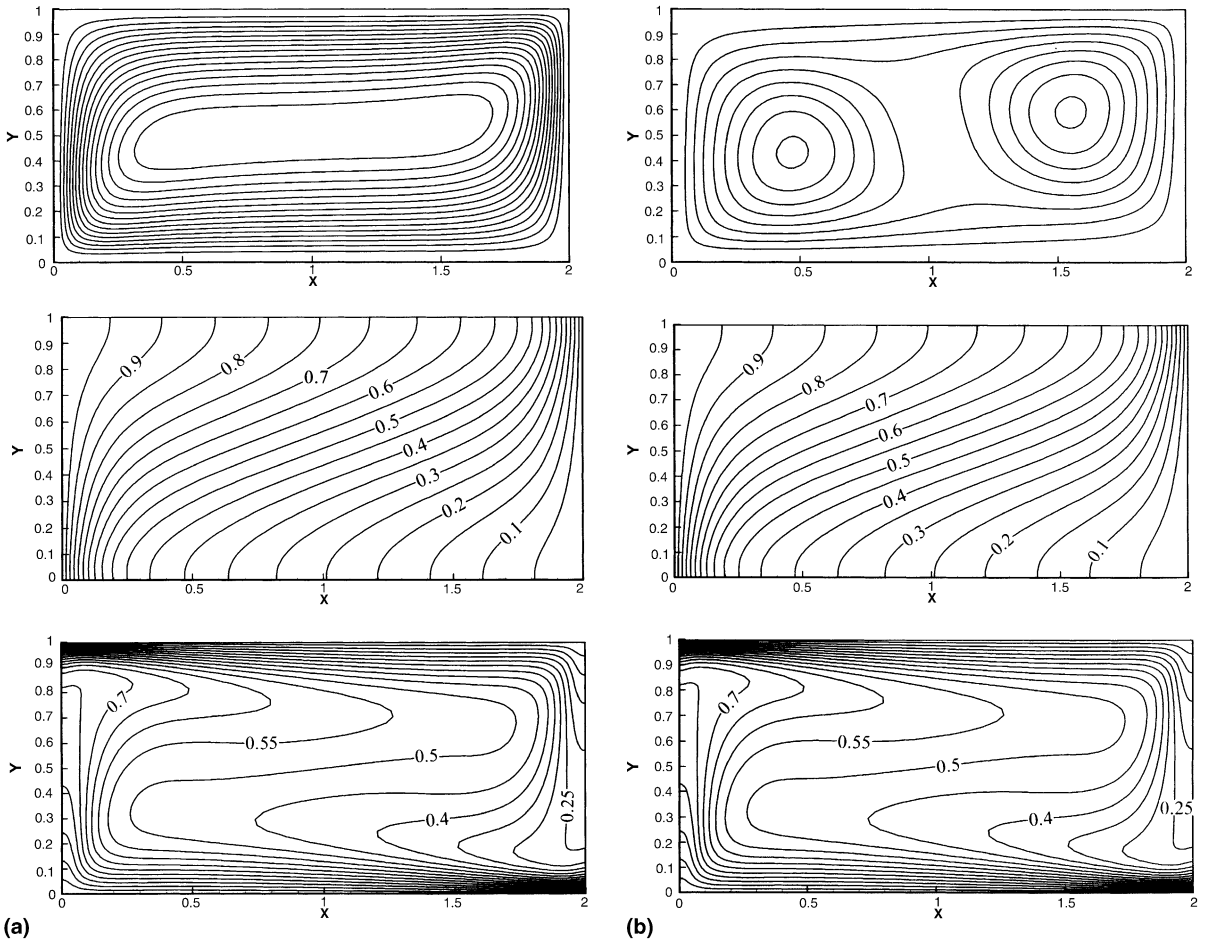

Fig. 2. Streamline (top), temperature (middle) and concentration (bottom) contours for two-dimensional and for different buoyancy ratios: (a) $N = 0$; (b) $N = -0.8$; (c) $N = -1.0$; (d) $N = -1.5$, $Ra_T = 10^5$, $Pr = 10$, $Le = 10$, $Da = 10^{-3}$.

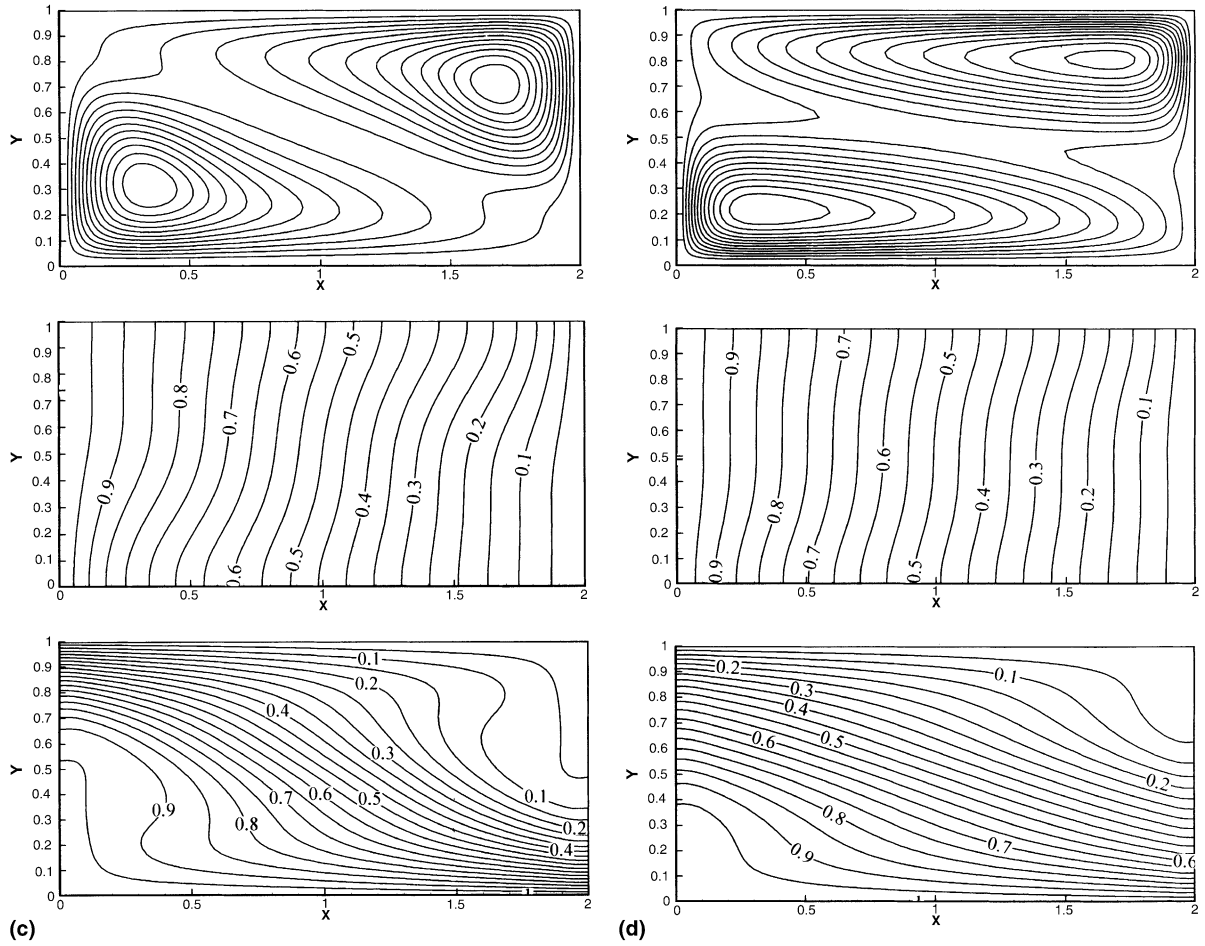

Fig. 2 (*continued*)

Landfill material decomposition due to bacterial activity produces flammable gases, which nearby heat sources may drive these gases to the heat source naturally. Renewable energy storage in stably stratified (salt solution) pool subjected to solar heating is efficient if the convection is prevented. Understanding the criteria for the onset of convection is very important in such a problem in order to improve thermal energy storage in solar ponds. Therefore, the present work can be justified academically and has some applications. In this work only stably stratified fluid is considered and there is work in progress on unstably stratified flow.

The paper focuses on the analysis of the flow, heat and mass transfer in a horizontal cavity of aspect ratio of two in longitudinal direction, which may resemble flow in a large enclosure. Prandtl number is fixed to 10 (aqueous solutions). The Lewis number is varied in the range of 1.0–1000 to cover wide range of species diffusion material in water. The work is concentrated on stable stratified flow. Two- and three-dimensional models were developed and the results of these models were compared. Interesting results were obtained for a wide range of solutal to thermal buoyancy ratios. The difference in the rate of heat and mass transfer between prediction of three- and two-dimensional simulations is not that significant, even though the flow exhibits three-dimensional structure. This is due to the fact that the spanwise flow is very weak compared with main flow.

2. Governing equations

A three-dimensional, steady state, incompressible laminar flow model is considered in the present study. All properties are assumed to be constant except that the effect of density variations on buoyancy is retained, by using the Boussinesq approximation. Also, Soret and Dufour effects are assumed to be negligible. The di-

mensionless governing equations based on the above assumptions are as follows:

Continuity

$$\nabla \cdot V = 0. \tag{1}$$

Momentum

$$0 = -\nabla P + \frac{Ra_T}{Pr}(\Theta + N\Phi)\boldsymbol{k} - \frac{1}{Da}V + \Gamma\nabla^2 V. \tag{2}$$

Energy

$$V \cdot \nabla\Theta = \frac{\Lambda}{Pr}\nabla^2\Theta. \tag{3}$$

Species conservation equation

$$V \cdot \nabla\Phi = \frac{\Lambda}{PrLe}\nabla^2\Phi. \tag{4}$$

The above equations are non-dimensionalized using L_Z, $(T_h - T_c)$, $(C_h - C_l)$, and v/L_Z as a length, temperature, species concentration and velocity, respectively. Hence, the non-dimensionalized variable can be defined as: $X = x/L_Z$, $Y = y/L_Z$, $Z = z/L_Z$, $P = pL^2/\rho v^2$, $U = uL_Z/v$, $V = vL_Z/v$, $W = wL_Z/v$, $\Theta = (T - T_C)/(T_H - T_C)$ and $\Phi = (C - C_l)/(C_h - C_l)$. The other non-dimensional parameters in the above equations are Prandtl number $Pr = v/\alpha$, thermal Rayleigh number $Ra_T = g\beta_T\Delta TL_Z^3/(v\alpha)$ the ratio of buoyancy forces, $N = Ra_S/Ra_T$, the solutal Rayleigh number, $Ra_S = g\beta_C(C_h - C_l)L_Z^3/(v\alpha)$, the Darcy number, $Da = K/L_Z^2$, the Lewis number, $Le = \alpha/D$. The parameters, g, k, K, β, v, and α refer to gravitational acceleration, unit vector in the vertical direction, permeability of the medium, coefficient of volumetric expansion, kinematics viscosity, and thermal diffusivity, respectively. Since the particle Reynolds number is less than unity, the Forchheimer term has been dropped

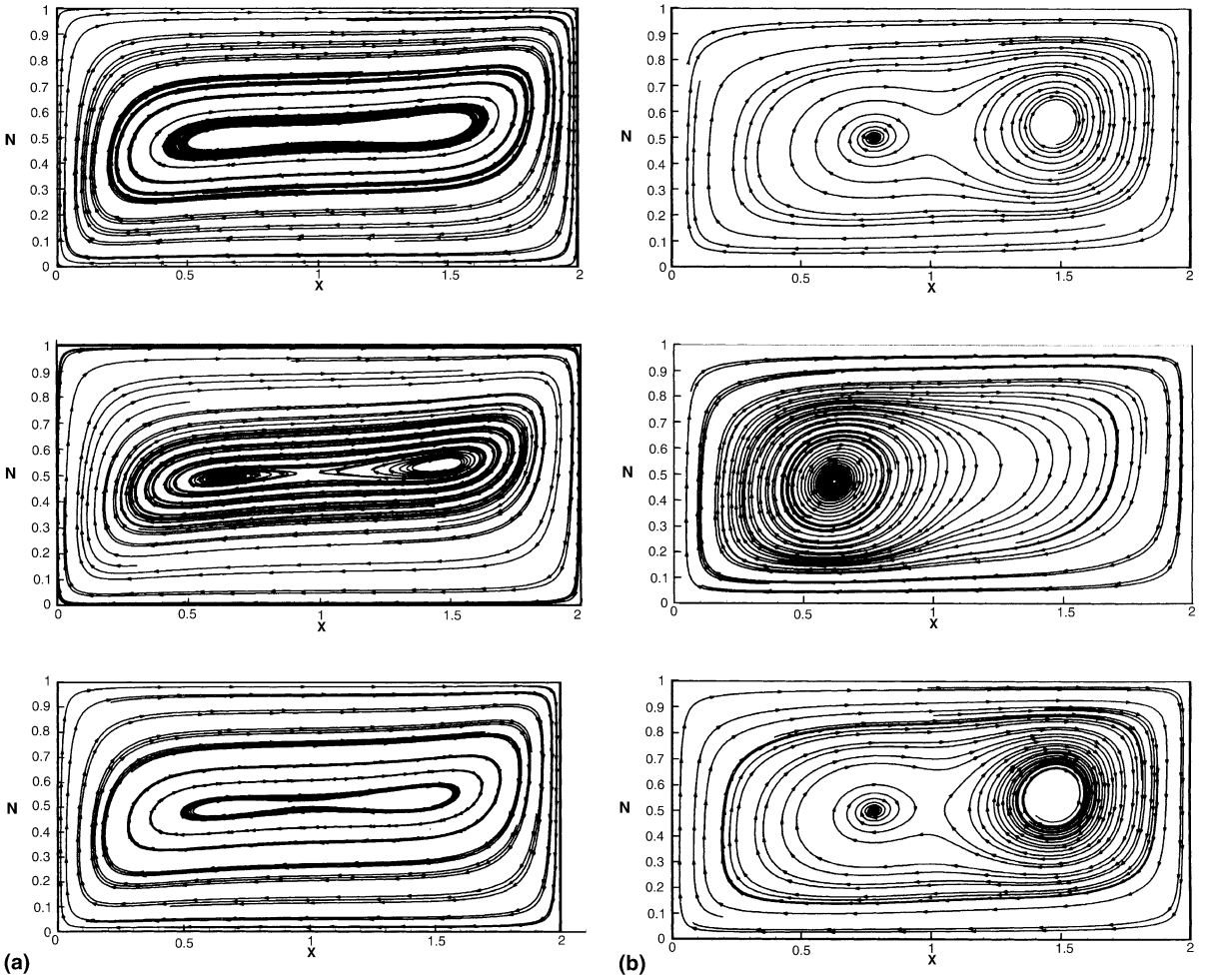

Fig. 3. Streamline contours for three-dimensional for transverse plax (X–Z) $X = 0.5$ (top), 1.0 (middle) and 1.5 (bottom) and for different buoyancy ratios: (a) $N = 0$; (b) $N = -0.8$; (c) $N = -1.0$; (d) $N = -1.5$; $Ra_T = 10^5$, $Pr = 10$, $Le = 10$, $Da = 10^{-3}$.

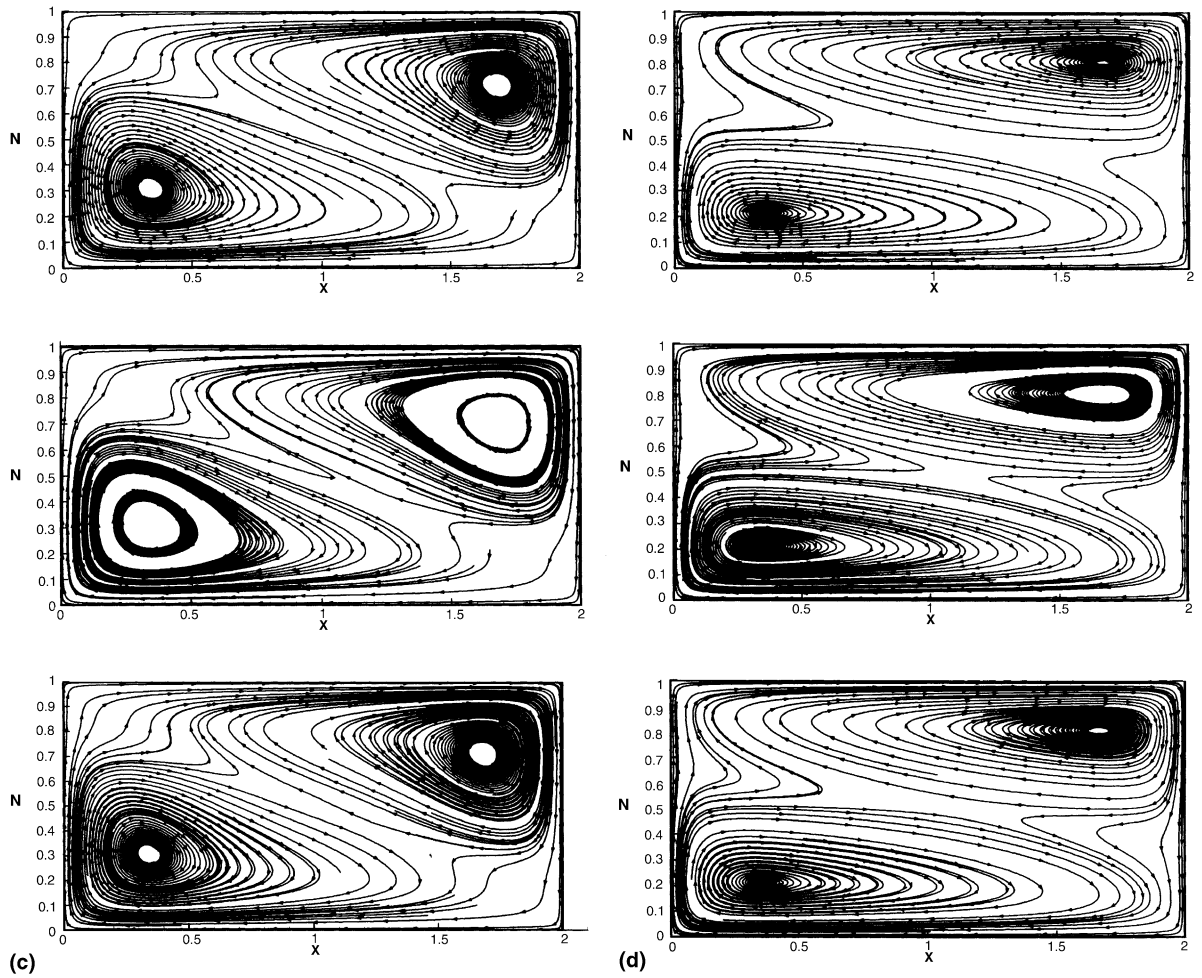

Fig. 3 (*continued*)

from the momentum equation (3) compared with Darcy and Brinkman terms. The ratio between effective viscosity and fluid viscosity, Γ, and the ratio of effective thermal conductivity to fluid thermal conductivity, Λ, are set to unity.

Boundary conditions for the velocity and temperature in non-dimensional form are as follows:

$$\text{for } X = 0, \quad \Theta = 1, \ \frac{\partial \Phi}{\partial X} = 0, \ U = V = W = 0 \tag{5a}$$

$$\text{for } X = L_X/L_Z, \quad \Theta = 0, \ \frac{\partial \Phi}{\partial X} = 0, \ U = V = W = 0 \tag{5b}$$

$$\text{for } Z = 0, \quad \Theta = 1, \ \frac{\partial \Theta}{\partial X} = 0, \ U = V = W = 0 \tag{5c}$$

$$\text{for } Z = 1, \quad \Theta = 0, \ \frac{\partial \Theta}{\partial X} = 0, \ U = V = W = 0 \tag{5d}$$

for $Y = 0$ and $Y = L_Y/L_Z$, non-slip condition applied for velocity components and heat and mass fluxes are set to zero.

3. Method of solution

Eqs. (1)–(4) and (5a)–(5d) are discretized using staggered, non-uniform control volumes. In order to minimize the numerical diffusion errors, a third order accurate QUICK scheme with flux limiter [17] is used in approximating the advection terms. The SIMPLE algorithm [18] is used to couple momentum and continuity equations. The momentum equations are solved by applying one iteration of the strongly implicit procedure (SIP) [19]. The discretization of the pressure correction equation results in a set of equations with a symmetric coefficient matrix which is solved by the conjugate gra-

dient (CG) method until the sum of absolute residuals has fallen by a factor of 10. On the other hand, the coefficient matrix of the set of equations resulting from the discretization of the energy equation is non-symmetric and solved iteratively by the BI-CGSTAB method [20]. SSOR preconditioning is used for accelerating the convergence rates of both the CG and the BI-CGSTAB methods. In most of the calculations presented here, a relaxation factor of 0.7 was applied to U, V, W, P, and T.

The use of iterative solution procedure efficiently removes only those Fourier components of the error whose wavelengths are smaller than or comparable to the grid spacing. The rate of convergence is high at the beginning of the calculation but it becomes worse after a few outer iterations. To reduce the high computer times inherent in the solution of three-dimensional natural convection problems, a full approximation storage (FAS) full multi-grid (FMG) method [5] applied to three-dimensional staggered grids is used to solve the problem which removes a wider spectrum of wavelengths efficiently. The equations are solved by a three level fixed V-cycle procedure starting at the coarsest grid and progressing to the finer grid level. For prolongation operations tri-linear interpolation is used for all variables. For restriction, the area weighted average procedure is used for all quantities defined on the

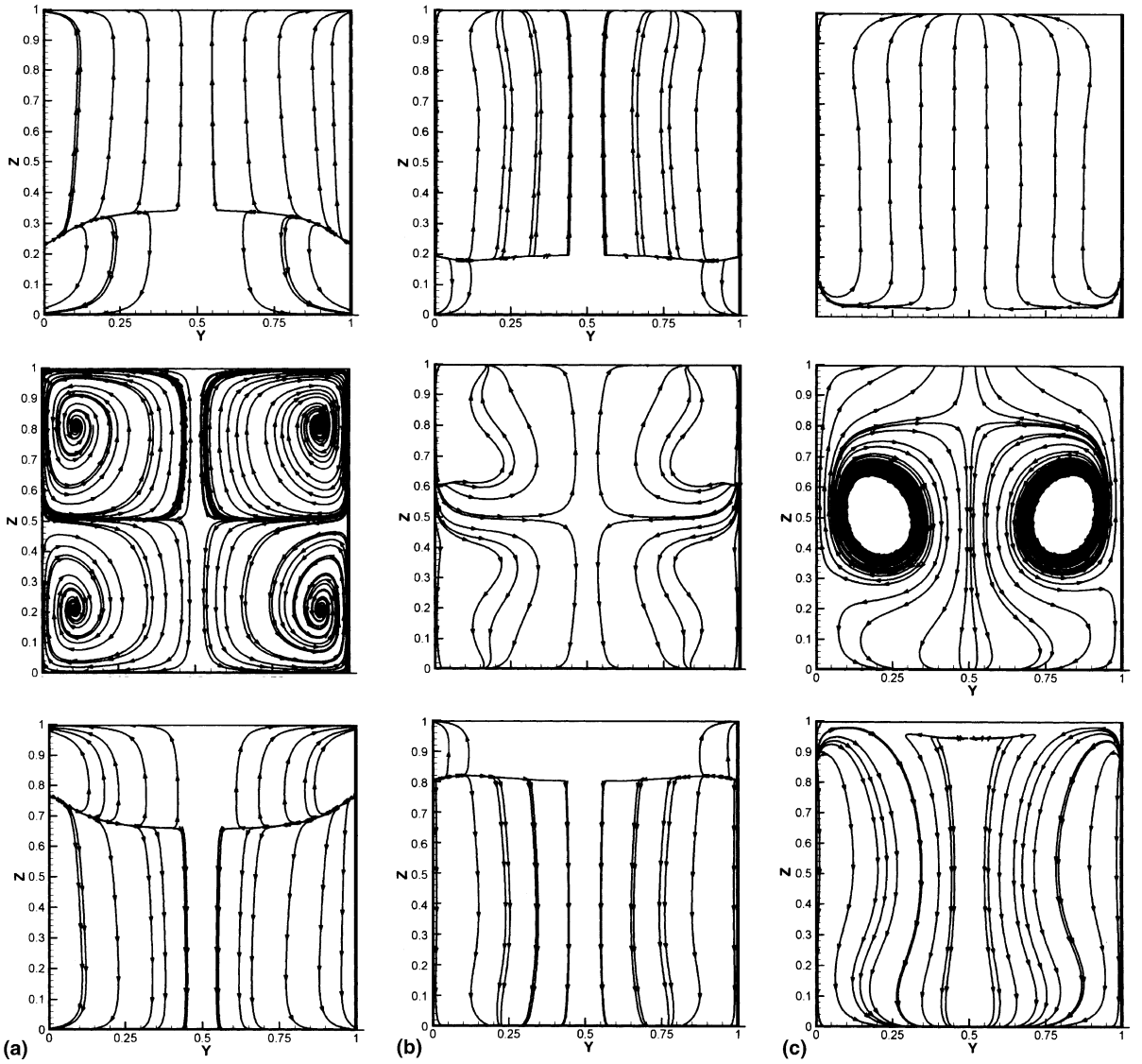

Fig. 4. Streamline contours for three-dimensional for $N = 0.0$, different transverse plan (Y–Z): (a) $X = 0.5$ (top), (b) $X = 1.0$ (middle) and (c) $X = 1.5$ (bottom); $Ra_T = 10^5$, $Pr = 10$, $Le = 10$, $Da = 10^{-3}$.

control-volume surface such as velocities. The volume weighted average procedure is adopted for all quantities defined at the control-volume center such as pressure and temperature.

In this work $82 \times 62 \times 62$ non-uniform grids are used on the finest level in the X, Y and Z directions. The non-uniform grids have denser clustering near the surface boundaries.

To ensure convergence of the numerical algorithm the following criterion is applied to all dependent variables over the solution domain:

$$\sum \left| \frac{\phi_{ijk}^{m} - \phi_{ijk}^{m-1}}{\phi_{ijk}^{m}} \right| \leqslant 10^{-3},$$

where ϕ represents a dependent variable U, V, W, P and T, the indexes i, j, k indicate a grid point; and the index m the current iteration at the finest grid lever. Also, the code is validated extensively for double diffusion problems and results were published elsewhere [5,21].

4. Results and discussion

Simulations were performed for two- and three-dimensional flows in an enclosure filled with saturated porous medium. The results of flow and heat and mass transfer characteristics of cross gradient double diffusion natural convection were investigated (Fig. 1). Vertically stabile stratified concentration gradient (negative gradient) is imposed on a differentially heated enclosure. The buoyancy ratio (concentration/temperature), N, is varied from thermal dominated flow ($N = 0$) to species concentration stabilizing flow condition $N = -2.0$. Also, the Lewis number (Le) is varied in the range of 1.0–1000 for a fixed Prandtl number ($Pr = 10.0$). The ranges of parameters which were used are typical for the salt intrusion to water and for solidification of ammonium chloride (NH_4Cl) and Na_2CO_3 solutions, where the Prandtl number ranges between 10 and 13 for these solutions. Benard et al. [14] gave the range of Lewis numbers for the mentioned solutions, Le in the range of 186–194. The Darcy number was varied from $Da = 10^{-3}$ to $Da = 10^{-5}$.

In the following sections, the effect of the buoyancy ratio, N, the modified Rayleigh number, Ra ($Ra_T Da$), and Lewis number is presented on the flow structure and on the rate of heat and mass transfer in the enclosure.

5. Effects of buoyancy ratio

The results of the flow structure for $Ra = 100$ ($Ra_T = 10^5$ and $Da = 10^{-3}$) and for $Le = 10$ are shown in Fig. 2 for two-dimensional simulations and for different buoyancy ratios. For $N = 0.0$, the flow is driven mainly by the thermal buoyancy force. The flow structure consists of only one main circulation occupying the entire enclosure. Concentration gradient reversal is evident at the core of the cavity, due to strong flow recirculation. As the $|N|$ value increases (in negative sense) the strength of the flow circulation decreases and starts to bifurcate into two weak circulations, Fig. 2(b). Also, concentration reversal diminishes as $|N|$ increases. At $N = -1$, the flow in the core of the cavity almost diminishes and flow channels along the boundaries. Heat transfer takes place mainly by conduction as evident from the isotherm distribution. For $N = -1.5$, a very weak flow along the boundaries is evident and the rate of transfer in the core is essentially diffusive.

Fig. 3 presents similar results for three-dimensional model. The figure illustrates the stream traces in the three transversal plans (X–Z) $Y = 0.25$, 0.5 and 0.75. It should be mentioned that there is a global similarity in bifurcation between the Figs. 2 and 3. For $N = 0$, the flow is solely driven by thermal buoyancy, which is symmetrical on the mid-X–Z plane. The flow is three-dimensional as it is revealed in Fig. 3(a), which shows stream traces on the transverse planes (X–Z planes). The parcel of particles that are traveling in the X–Z plane did not stay on the same plane, where a weak spiral flow is evident, Fig. 4(a), which shows the stream traces on the transverse planes (Y–Z) for $N = 0$. The formation of such a spiral flow may be because of the effect of lateral boundaries and three-dimensional boundary layer formations at the corners of the enclosure. Experimental and numerical results for flow in a differentially heated

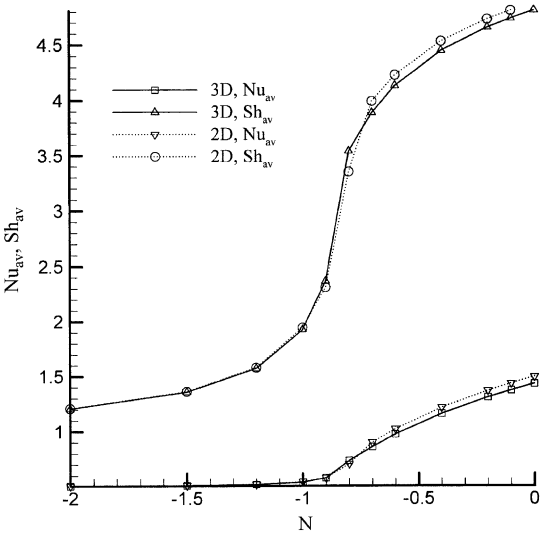

Fig. 5. The effect of N on Nu and Sh for two-dimensional and three-dimensional models, ($Ra_T = 10^5$, $Pr = 10$, $Le = 10$, $Da = 10^{-3}$).

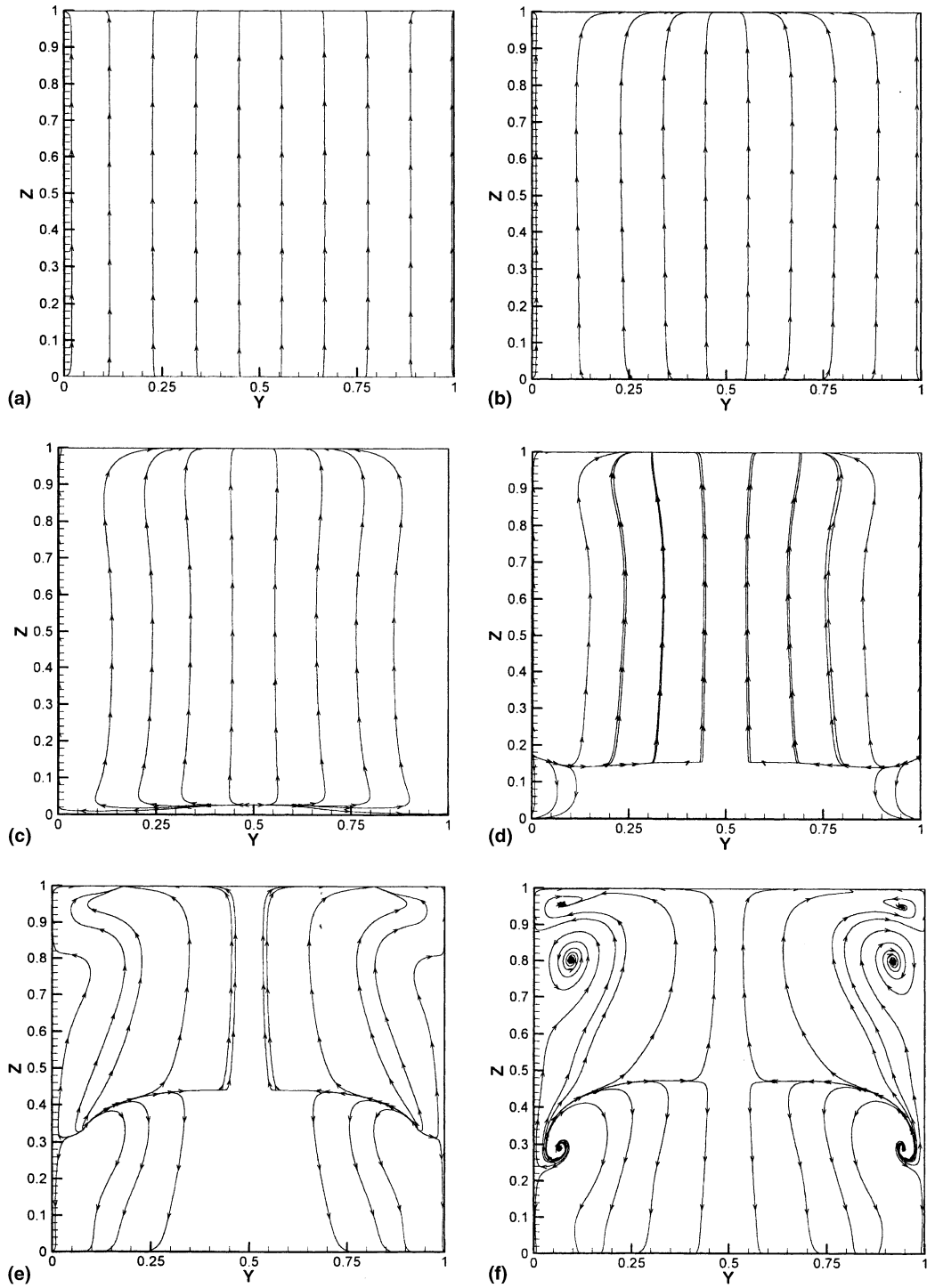

Fig. 6. Streamline contours for transverse plan (Y–Z) $X = 0.5$ and for different Rayleighs: (a) $Ra = 1.0$, (b) $Ra = 10.0$, (c) $Ra = 60.0$, (d) $Ra = 100.0$, (e) $Ra = 400.0$ and (f) $Ra = 1000.0$; $Pr = 10$, $N = -0.5$, $Le = 10$, $Da = 10^{-3}$.

cubic cavity [22,23] without solutal effects showed similar results. They found that the spiral flow is sensitive to the lateral boundary conditions. These findings support the idea that the effect of lateral boundaries and

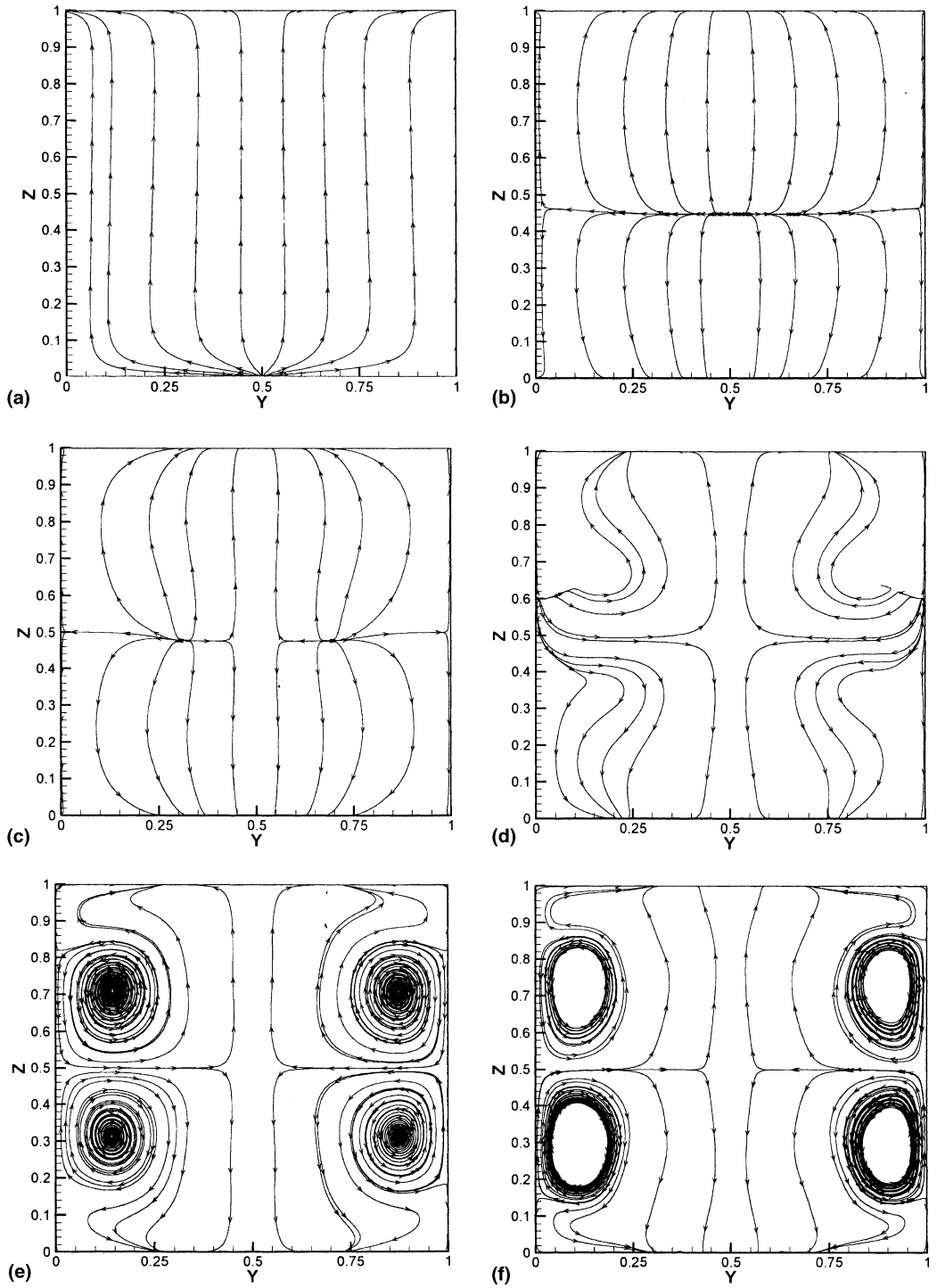

Fig. 7. Streamline contours for transverse plan (Y–Z) $X = 1.0$ and for different Rayleighs: (a) $Ra = 1.0$, (b) $Ra = 10.0$, (c) $Ra = 60.0$, (d) $Ra = 100.0$, (e) $Ra = 400.0$ and (f) $Ra = 1000.0$; $N = -0.5$, $Pr = 10$, $Le = 10$, $Da = 10^{-3}$.

three-dimensional boundary layer formations at the corners is the main cause of the spiral flows.

For $|N| > 0.0$, the effect of concentration is to resist the vertical flow, where the ascending (descending) flow

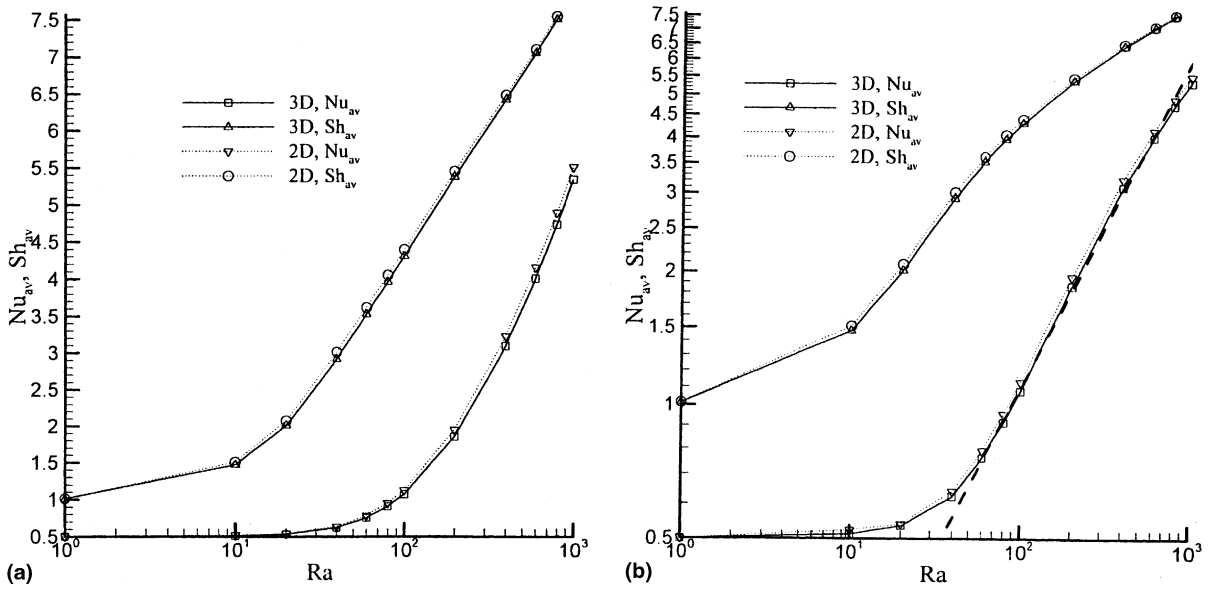

Fig. 8. The effect of *Ra* on *Nu* and *Sh* for two-dimensional and three-dimensional models, for $N = -0.5$, ($Pr = 10$, $Le = 10$, $Da = 10^{-3}$): (a) semi-log scale and (b) log-scale.

has higher (lower) density compared with the case of $N = 0$, which needs more energy to be carried. Therefore, the strength of spiral flow decreases (Fig. 4(b)). Also, the dynamics of the flow changes and distance between two groups of spiraling particles diminishes as N increases (in negative sense) from 0 to −0.4. When the buoyancy forces of the thermal and species concentration become of the same order of magnitude, the flow started to bifurcate and complex flow patterns were predicted. Yet for $N = -0.7$, the transverse flow structures show perfect symmetry along the central plane ($X = 1.0$) with the "eyes" of the spiraling flow at the center plane Y–Z moving toward the core of the enclosure, while the main flow is ascending and descending at the right and left planes, respectively (Fig. 4(c)). The flow structure becomes very complex at $N = -0.8$ and the symmetry is lost due to the formation of internal waves as predicted by Bennacer et al. [16]. Even though the solution was fully converged, it is expected that the flow experiences a weak instability. The transverse secondary flows are so weak compared with the main flow; therefore the convergence of the solution was not that sensitive to the formation of a secondary flow. Also, the difference between predictions of three-dimensional and two-dimensional models of the rate of heat and mass transfer is not that significant, which will be discussed later on. At $N = -1.0$, the flow bifurcates into two main circulations, Fig. 3(c). The horizontal trajectory of the fluid particles rising along the hot wall decreases as the N, stabilizing force, increases. As $|N|$ approaches unity (in negative sense), the heavy fluid parcel (high concentration) of particles sinks before they arrive at the other end of the enclosure, therefore two main recirculation forms. Since, the particles near the hot wall have low density compared with particles away from the hot wall, it is expected that the hot particles may reach higher altitude before they descend. In fact some particles, which are very near to the hot wall, successfully reach

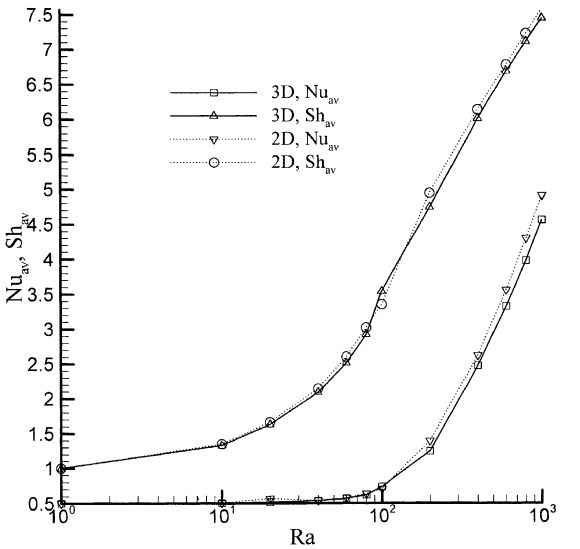

Fig. 9. The effect of *Ra* on *Nu* and *Sh* for two-dimensional and three-dimensional models, for $N = -0.8$, ($Pr = 10$, $Le = 10$, $Da = 10^{-3}$).

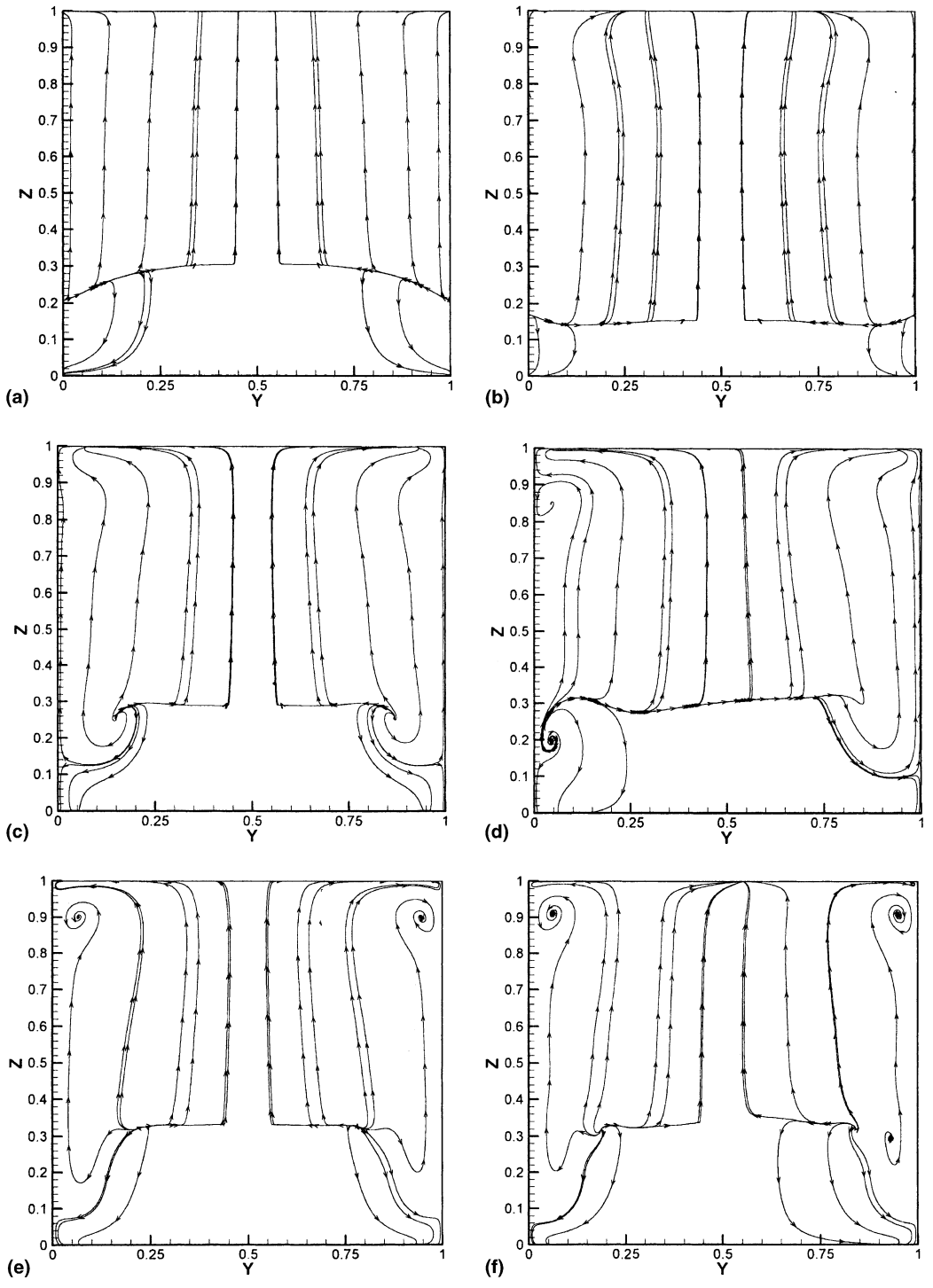

(I)

Fig. 10. Streamline contours and for different Le numbers: (a) $Le = 1.0$, (b) $Le = 10.0$, (c) $Le = 60.0$, (d) $Le = 100.0$, (e) $Le = 400.0$ and (f) $Le = 1000.0$; for transverse plan (Y–Z) (I) $X = 0.5$ and (II) $X = 1.0$ ($N = -0.5$, $Pr = 10$, $Da = 10^{-3}$).

the other end of the enclosure. Similar discussion is valid for the cold end of the enclosure as a result of the skew symmetry of the problem. For $N = -1.5$, the flow almost separated into two main thermally induced

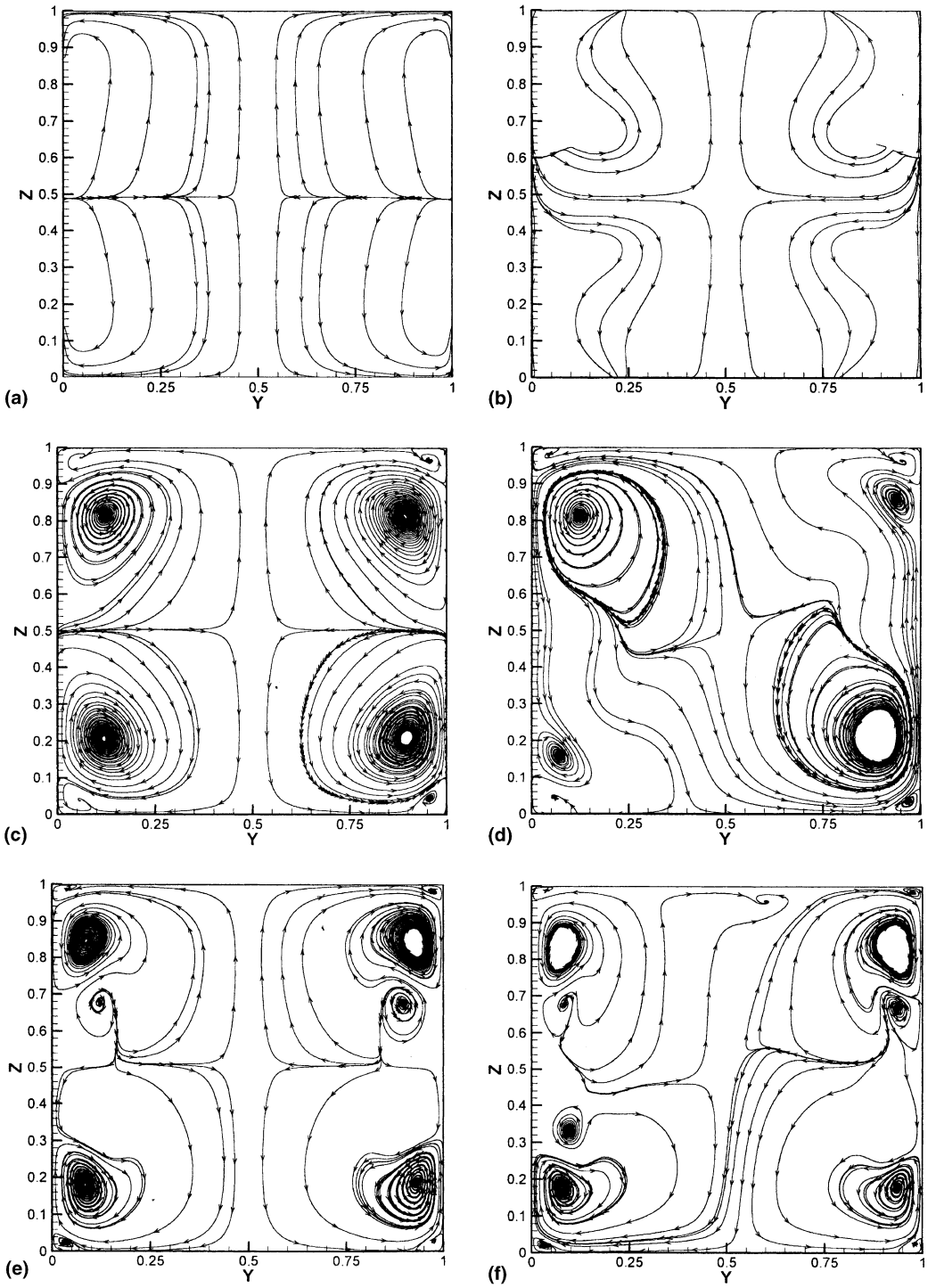

(II)

Fig. 10 (*continued*)

circulations. The reverse flow is mainly due to the difference in time diffusion between energy and species.

The effect of buoyancy ratio on the average rate of heat and mass transfer is shown in Fig. 5 for $Ra = 100$

and $Le = 10$. For $|N| \geqslant 1.0$ the heat transfer is diffusive, while mass transfer enhanced by advection of the momentum due to thermally induced circulations. The difference between two- and three-dimensional simulations is not that significant because the secondary flow is very weak compared with main flow. Usually, the results of heat and mass transfer for two-dimensional simulation are slightly higher than the three-dimensional results. This difference can be attributed to the effect of the lateral boundary and flow conditions at the corners of the enclosure, where the shear force resists flow motion. For N about -0.8 the three-dimensional simulation slightly overpredicts the rate of transfer, where the flow bifurcation takes place and flow mixing enhances.

6. Effect of Rayleigh number

Figs. 6 and 7 show stream traces in transverse plane (Y–Z) for $X = 1/2$ and $X = 1.0$, respectively, for different Rayleigh numbers and for $Le = 10$ and $N = -0.5$. The complexity of the flow increases with Ra. The flow is strictly two-dimensional for $Ra = 1.0$ and slightly three-dimensional for $Ra = 10$. The flow preserves the symmetry for all values of Ra investigated. Four transverse secondary spiral flows become evident for $Ra \geqslant 400$. Figs. 8(a) and (b) represent the heat and mass transfer in semi-log and log scales, respectively. The heat transfer is diffusive for $Ra < 10$ (Fig. 8(a)). As mentioned before, the effect of thermally induced flow enhances the rate of mass transfer. The rate of mass transfer can be correlated as $Sh_{av} = a \log Ra + b$ for $Ra > 20$, which does not follow the boundary layer flow correlations. The rate of heat transfer can be correlated as $Nu_{av} = aRa^n$ for $Ra > 60$ as shown Fig. 8(b), which follows the boundary layer flow correlation. Fig. 9 shows Nu and Sh as a function of Rayleigh number for $N = -0.8$. As mentioned before the flow bifurcation becomes evident, the rate of heat and mass transfer is higher that that for $N = -0.5$ (Fig. 8), but the trend is the same for both N values.

7. Effect of Lewis number

Figs. 10(I) and (II) show the stream trace lines for $X = 1/2$ and $X = 1$, respectively, on the transverse plane Z–Y. For $Ra = 100$, the flow is three-dimensional for all the range of Le numbers. The flow preserves symmetry along plane (X–Z) for the investigated range of Le but becomes complex for $Le \geqslant 400$. The flow mainly consists four spiral secondary vortices superimposed on the main flow. The effect of Le on the rate of heat and mass transfer is illustrated in Figs. 11(a) and (b) for $N = -0.5$ and $N = -0.8$, respectively. The influence of Le on the rate of heat transfer is not that significant, i.e., the effect of Le on the thickness of the thermal boundary layer is not that considerable. While increasing Le increases the rate of mass transfer as expected. The effect of N values

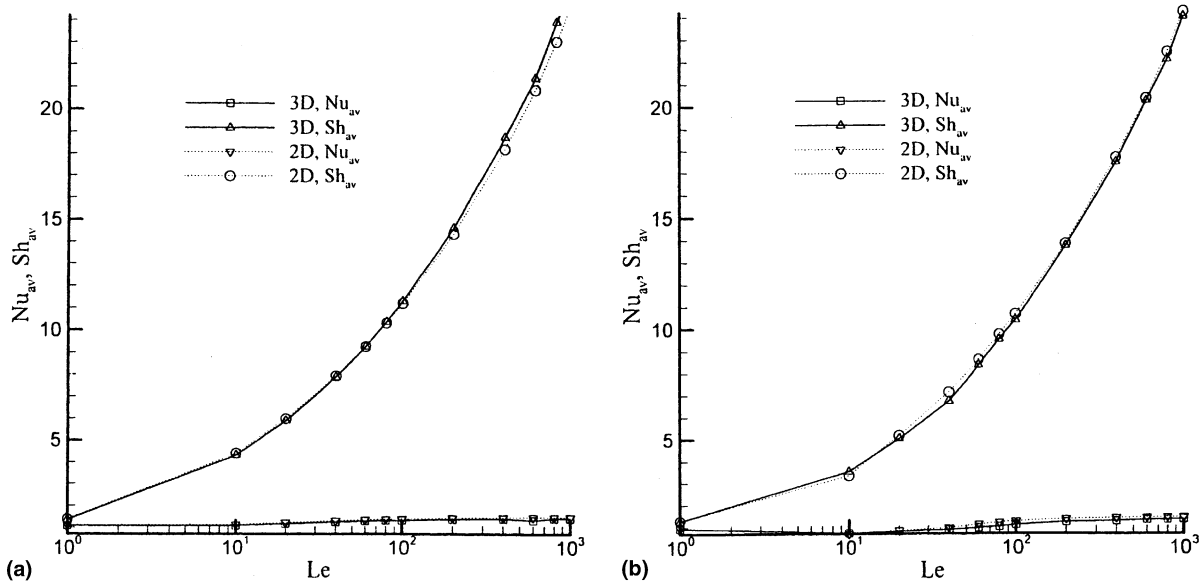

Fig. 11. The effect of Le on Nu and Sh for two-dimensional and three-dimensional models for (a) $N = -0.5$ and (b) $N = -0.8$, ($Pr = 10$, $Da = 10^{-3}$).

at least for values of −0.5 and −0.8 is weak on the rate of mass transfer.

8. Conclusions

Two- and three-dimensional models are presented for flow in an enclosure heated differentially and stably stratified in imposed vertically. The effects of the main controlling parameters, such as buoyancy ratio, porous Rayleigh number, Lewis number, were investigated to gain new insights into formation of flow patterns and into the rate of heat and mass transfer. The main findings of the present work can be summarized as follows:

(1) The difference between two- and three-dimensional models is not that significant as far as heat and mass transfer is concerned.
(2) The flow structure mainly consists of thermally induced recirculation flow superimposed with weak secondary, spiraling flow in transverse direction. However, when N becomes an order of magnitude of unity (about −0.8) the flow bifurcates into two thermally driven circulations. Further increasing N (greater than unity, in negative sense) the flow stabilizes and main circulations diminish in the strength.
(3) Unstable flow is predicted for $Le = 100$ due to internal wave formation for N greater than −0.8. This was evident for two- and three-dimensional models.
(4) In general, a two-dimensional model is sufficient enough to properly model the rate of heat and mass transfer, at least for the range of investigated parameters.

Acknowledgements

The first author gratefully acknowledges the support of the Natural Sciences and Engineering Research Council of Canada (NSERC) through the research grant.

References

[1] D.A. Nield, A. Bejan, Convection in Porous Medium, Springer, New York, 1999.
[2] F. Alavyoon, On natural convection in vertical porous enclosures due to prescribed fluxes of heat and mass transfer at the vertical boundaries, Int. J. Heat Mass Transfer 36 (1993) 2479–2498.
[3] M. Mamou, P. Vasseur, E. Bilgen, Multiple solution for double-diffusive convection on a vertical porous enclosure, Int. J. Heat Mass Transfer 38 (1995) 1787–1798.
[4] M. Nishimura, M. Wakamatsu, A.M. Morega, Oscillatory double-diffusive convection in a rectangular enclosure with combined horizontal temperature and concentration gradients, Int. J. Heat Mass Transfer 41 (1998) 1601–1611.
[5] I. Sezai, A.A. Mohamad, Three-dimensional double-diffusive convection in a porous cubic enclosure due to opposing gradients of temperature and concentration, J. Fluid Mech. 400 (1999) 333–353.
[6] D.A. Nield, Onset of thermohaline convection in a porous medium, Water Resour. Res. 4 (1968) 553–560.
[7] O.V. Trevisan, A. Bejan, Natural convection with combined heat and mass transfer buoyancy effects in a porous medium, Int. J. Heat Mass Transfer 28 (9) (1985) 1597–1611.
[8] O.V. Trevisan, A. Bejan, Mass and heat transfer by natural convection in a vertical slot filled with porous medium, Int. J. Heat Mass Transfer 29 (1986) 403–415.
[9] O.V. Trevisan, A. Bejan, Mass and heat transfer by high Rayleigh number convection in a porous medium heated from below, Int. J. Heat Mass Transfer 30 (1987) 2341–2356.
[10] M. Mamou, P. Vasseur, E. Bilgen, Double diffusive convection instability in a vertical porous enclosure, J. Fluid Mech. 368 (1998) 263–289.
[11] P. Nithiarasu, K.N. Seetharamu, T. Sundarajan, Double-diffusive natural convection in an enclosure filled with fluid-saturated porous medium: a general non-Darcy approach, Numer. Heat Transfer A 30 (1996) 413–426.
[12] B. Goyeau, J.-P. Songbe, D. Gobin, Numerical study of double-diffusive natural convecton in a porous cavity using the Darcy–Brinkman formulation, Int. J. Heat Mass Transfer 39 (1996) 1363–1378.
[13] M. Karimi-Fard, M.C. Charrier-Mojtabi, K. Vafai, Non-Darcian effects on double-diffusive convection within a porous medium, Numer. Heat Transfer A 31 (1997) 837–852.
[14] C. Benard, R. Benard, R. Bennacer, D. Gobin, Melting driven thermohaline convection, Phys. Fluids 8 (1996) 112–130.
[15] A.A. Mohamad, R. Bennacer, Natural convection in a confined saturated porous medium with horizontal temperature and vertical solutal gradients, Int. J. Thermal Sci. 40 (2001) 82–93.
[16] R. Bennacer, A.A. Mohamad, D. Akrour, Transient natural convection in an enclosure with horizontal temeprature and vertical solutal gradients, Int. J. Thermal Sci. 40 (2001) 899–910.
[17] B.P. Leonard, S. Mokhtari, Beyond first order upwinding: the ULTRA-SHARP alternative for nonoscillatory steady-state simulation of convection, Int. J. Numer. Meth. Eng. 30 (1990) 729–766.
[18] S.V. Patankar, Numerical Heat Transfer and Fluid Flow, McGraw-Hill, New York, 1980.
[19] H.L. Stone, Iterative solution of implicit approximations of multi-dimensional partial differential equations, SIAM J. Numer. Anal. 5 (1968) 530–558.
[20] H.A. Van Der Vorst, BiCGSTAB: a fast and smoothly converging variant of Bi–CG for the solution of non-symmetric linear systems, SIAM J. Sci. Stat. Comput. 13 (1992) 631–644.

[21] I. Sezai, A.A. Mohamad, Double diffusive convection in a cubic enclosure with opposing temperature and concentration gradient, Phys. Fluids 12 (9) (2000) 2210–2223.
[22] L. Leonardi, T.A. Kowalewski, V. Timchenko, G. de Vahl Davis, Effects of finite wall conductivity on flow structure in natural convection, in: A.A. Mohamad, I. Sazai (Eds.), CHMT99, Proceedings of the International Conference on Computational Heat and Mass Transfer, Famagusta, Mersion 10, Turkey, 1999, pp. 182–188.
[23] W.J. Hiller, St. Koch, T.A. Towalewski, Three-dimensional structures in laminar natural convection in a cube enclosure, Exp. Thermal Fluid Sci. 2 (1989) 34–44.